Supplementary Information

Growth-Coupled Biosorption and Metabolic Regulation Enable Efficient Copper Bioremediation by *Aspergillus foveolatus* FX

World Journal of Microbiology and Biotechnology

Longteng Fang[1,2], Jing Jing[1], Liping Xu[1,2], Shuai He[2], Rayhan Xayabbas[2], Reziyamu Wufuer[1], Ayitila Maimaitijiang[1*], Zhiwei Zhang[1*]

[1] School of Pharmaceutical Sciences and Institute of Materia Medica, Xinjiang University, Urumqi, Xinjiang, China

[2] School of Life Science and Technology, Xinjiang University, Urumqi, Xinjiang, China

***Correspondence:** Ayitila Maimaitijiang, ayitila@xju.edu.cn; Zhiwei Zhang, zhangzzw@xju.edu.cn

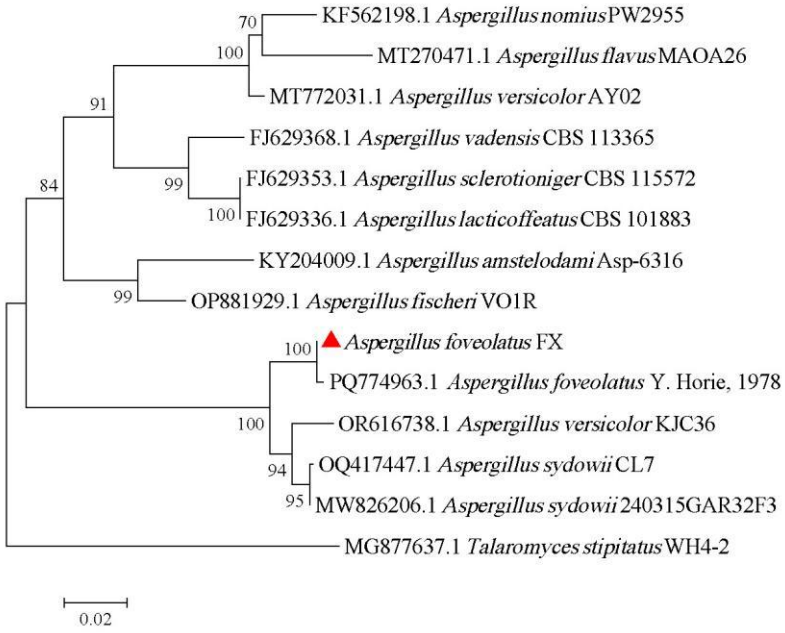

Fig. S1 ITS rDNA-based phylogeny of *A. foveolatus* FX. The neighbour-joining tree was generated with 1000 bootstrap replicates. The red triangle marks strain FX. Scale bar, 0.02 substitutions per site.

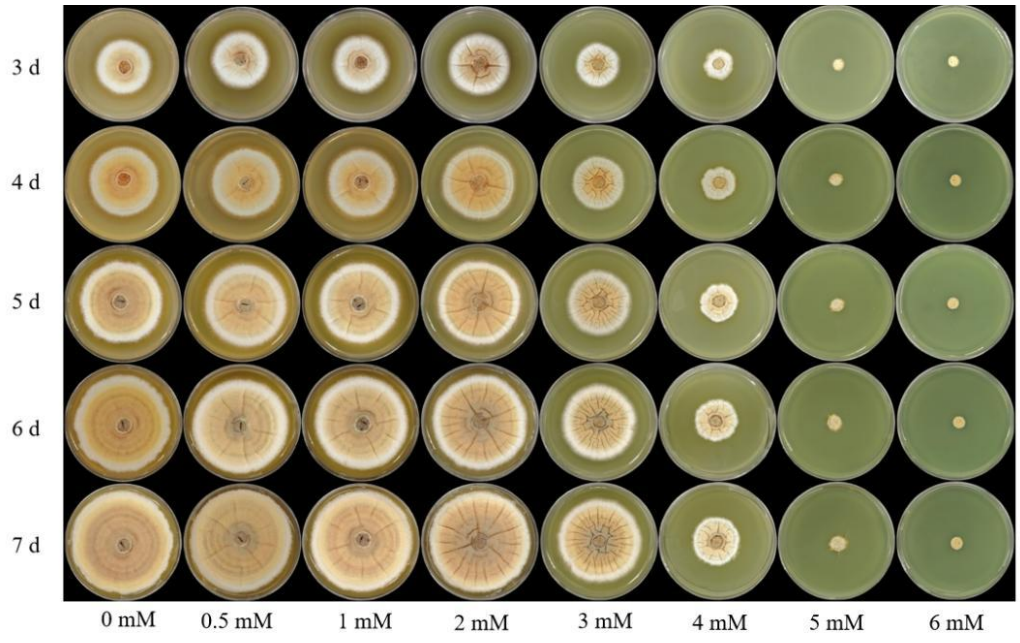

Fig. S2 Colony morphology of *A. foveolatus* FX grown on medium supplemented with different concentrations of Cu for 3–7 d.

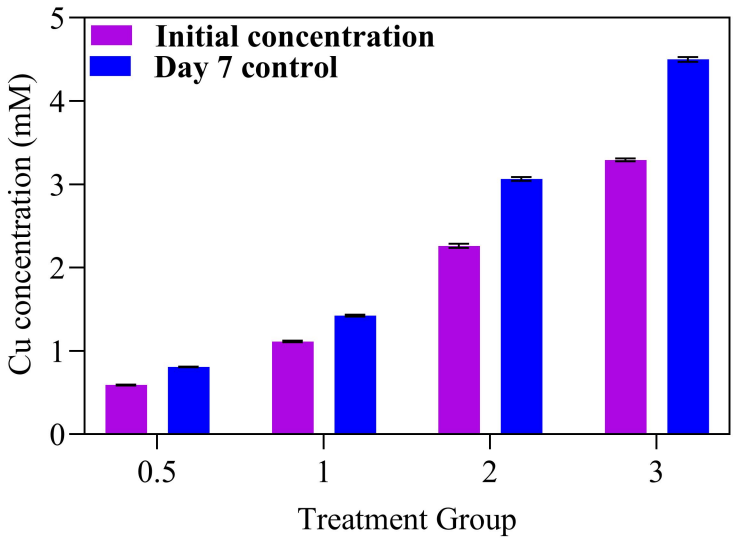

Fig. S3 Initial and residual Cu concentrations after 7 d in control samples across different initial Cu concentration treatments.

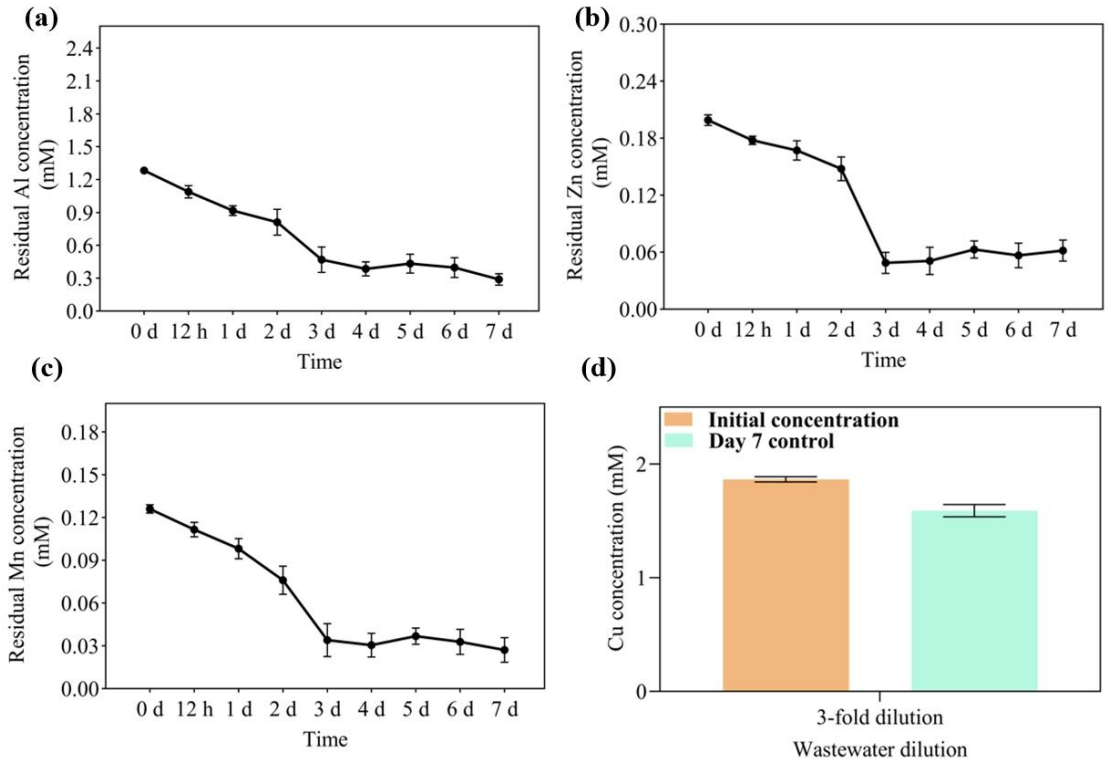

Fig. S4 Metal removal performance of *A. foveolatus* FX in diluted copper mine wastewater: residual (a) Al, (b) Zn, and (c) Mn concentrations over time, and (d) initial and residual Cu concentrations after 7 d in control samples.

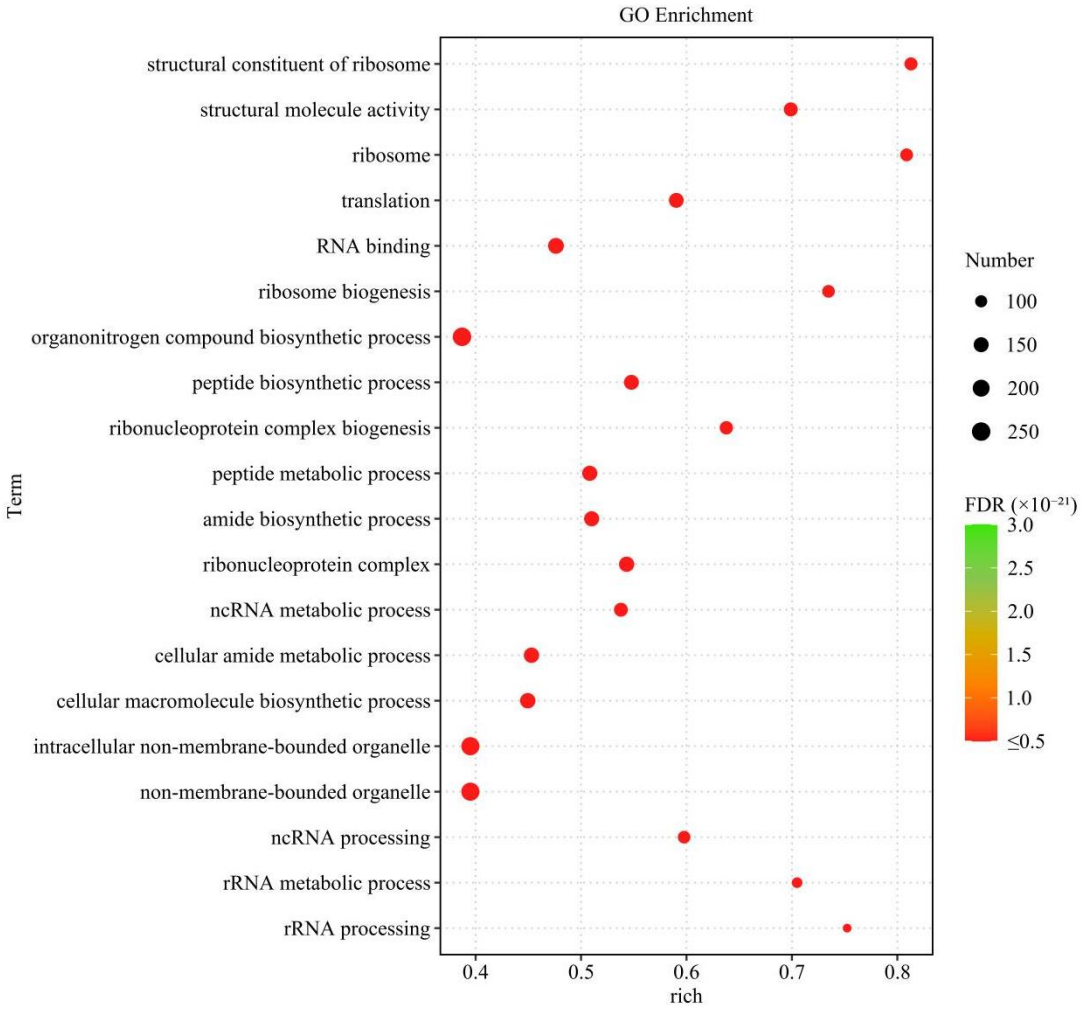

Fig. S5 GO enrichment analysis of upregulated DEGs in *A. foveolatus* FX under Cu stress.

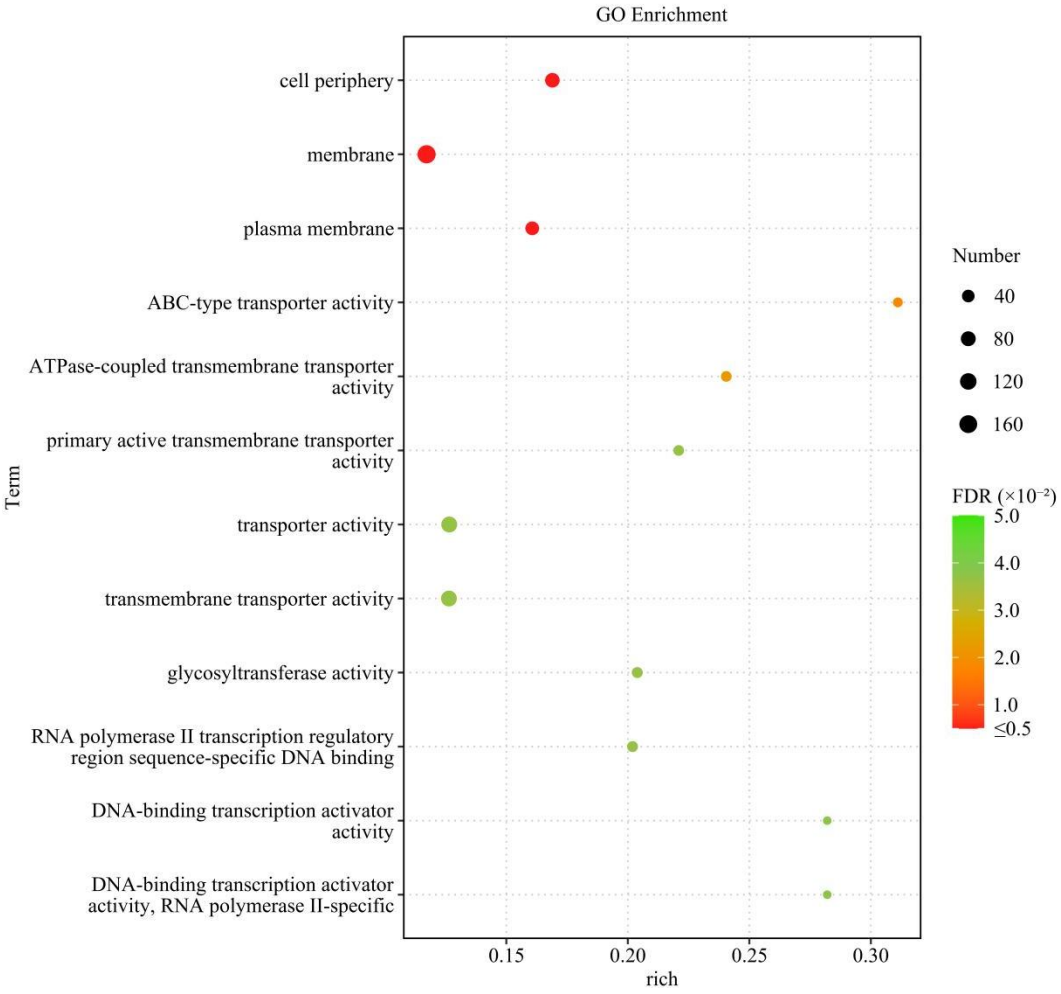

Fig. S6 GO enrichment analysis of downregulated DEGs in *A. foveolatus* FX under Cu stress.

Structural determination of secondary metabolites of *A. foveolatus* FX

N,N',N''-triacetylfusarinine C (**1)** obtained as a yellow amorphous solid, analysis of the 1D and HSQC spectra assorted 13 carbon resonances to three carbonyl carbons (δ_C 172.6, 170.2, 159.7), one non-protonated sp^2 carbon (δ_C 148.7), one sp^2 methine (δ_C 114.4), two sp^3 oxymethylenes (δ_C 62.2, 48.6), one sp^3 methine (δ_C 51.0), three sp^3 methylenes (δ_C 32.9, 28.7, 21.8), and two methyl groups (δ_C 24.1, 23.1). COSY analysis established the contiguous proton spin systems, revealing the exchangeable proton NH7 (δ_H 6.29) with C7–C8–C9–C10 chain and the oxygen-bridged C4–C5 moiety. HMBC correlations further confirmed the connectivity between structural fragments and key functional groups, including those from H2 to C1, from H3 to C2/C3/C4, and from H5 to C6, confirming the –CH_2–O–CO– ester linkage. Additionally, HMBC signals from the NH7 and H12 to C11 confirmed the intramolecular peptide bond. Mass spectrometry analysis showed a TOF-MS peak at m/z 851.42 $[M - H]^-$. Comparison with reported data identified the compound as N,N',N''-triacetylfusarinine C (TAFC), which consists of three N-acetylfusarinine units (Walsh et al. 2021).

Further NMR analysis of the Al^{3+} N,N',N''-triacetylfusarinine C (**2)** revealed that its ^1H NMR spectrum was highly similar to that of free TAFC, whereas the ^{13}C NMR spectrum was poorly resolved. Fortunately, mass spectrometry exhibited a peak at m/z 899.36 $[M + Na]^+$, and comparison with publications identified the compound as the Al^{3+}-TAFC coordination (Novák et al. 2017). Similarly, the Fe^{3+}-TAFC (**3)** coordination did not yield clear NMR data; however, MS analysis showed m/z 928.31 $[M + Na]^+$, leading to its identification as the Fe^{3+}-TAFC complex upon comparison with reported data (Huang et al. 2020).

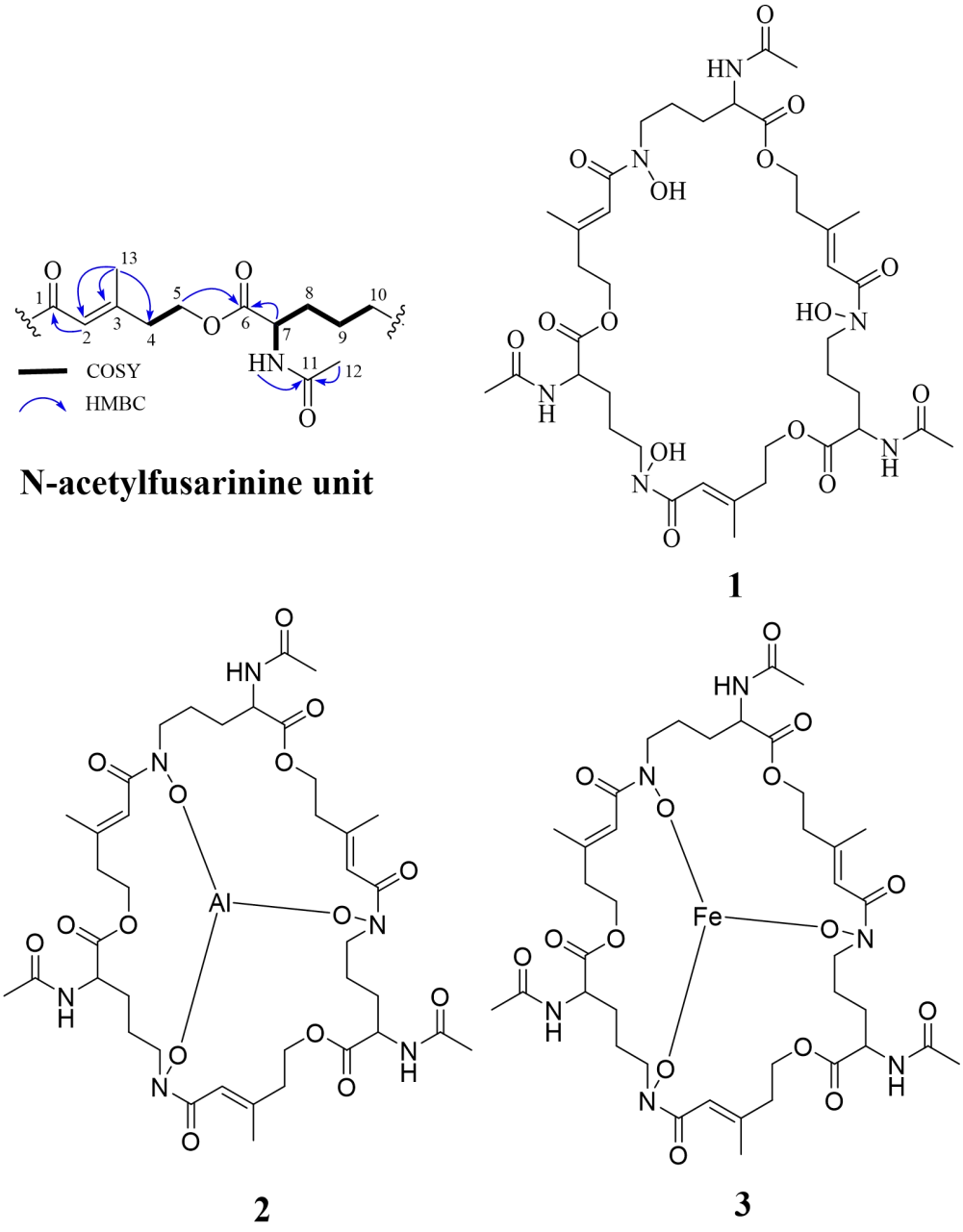

Fig. S7 Key COSY and HMBC correlations of the N-acetylfusarinine unit and structures of compounds **1–3**.

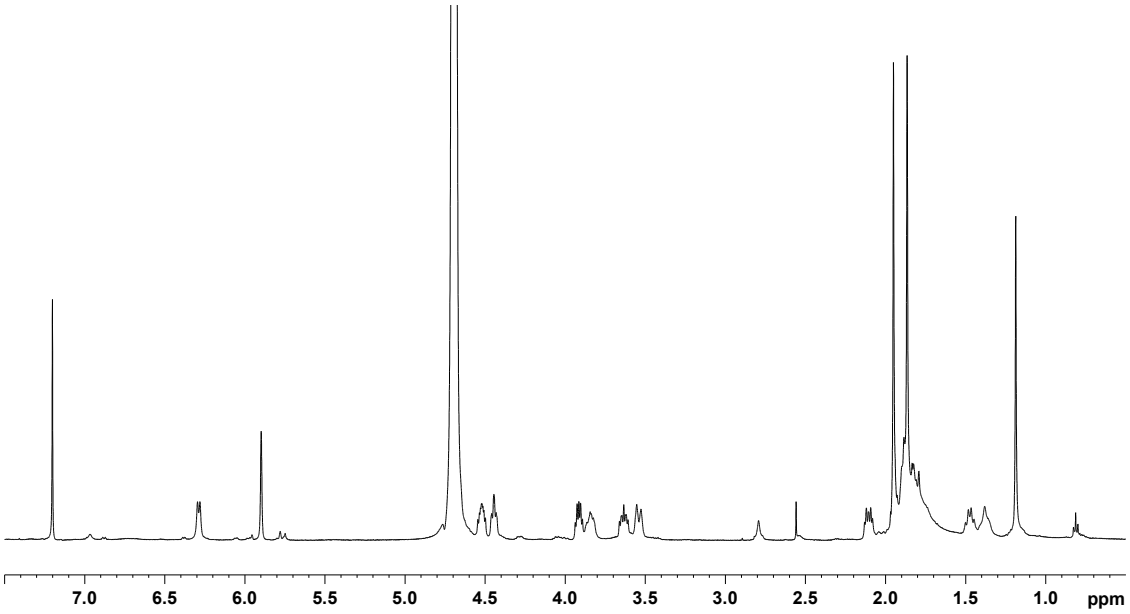

Fig. S8 ^{1}H NMR spectrum of **1** (500 MHz, $CDCl_3$).

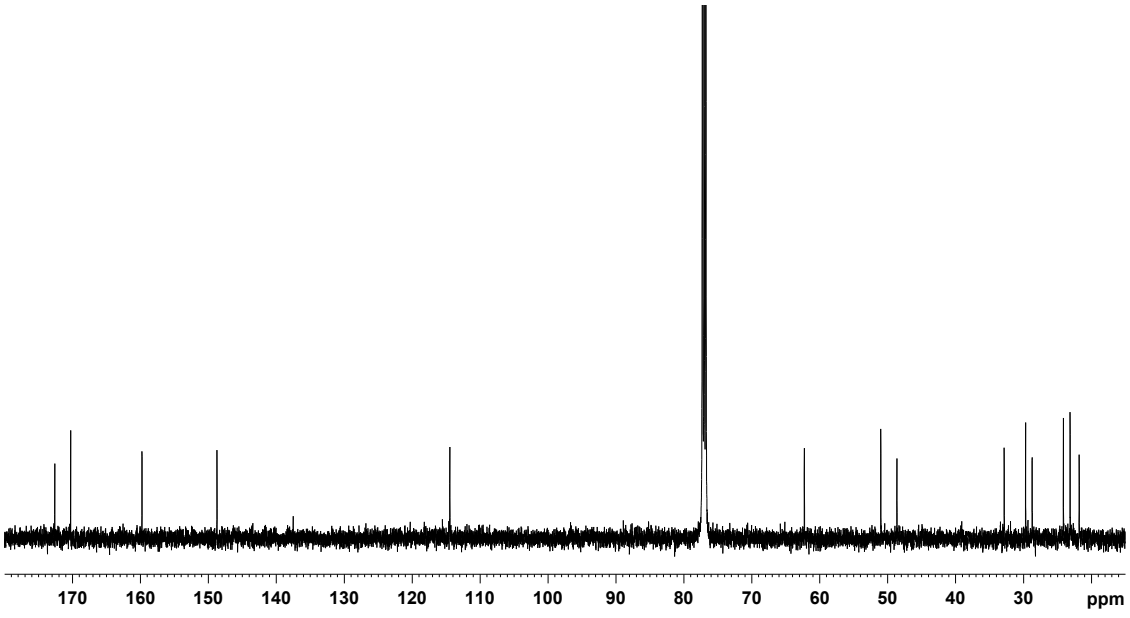

Fig. S9 ^{13}C NMR spectrum of **1** (125 MHz, $CDCl_3$).

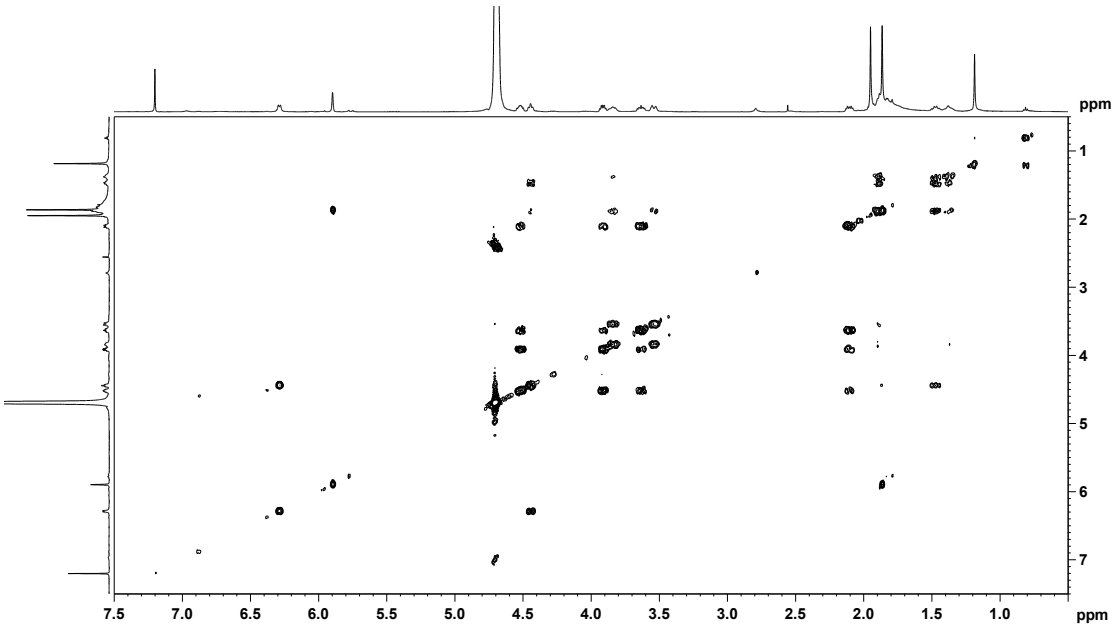

Fig. S10 COSY spectrum of **1** (500 MHz, $CDCl_3$).

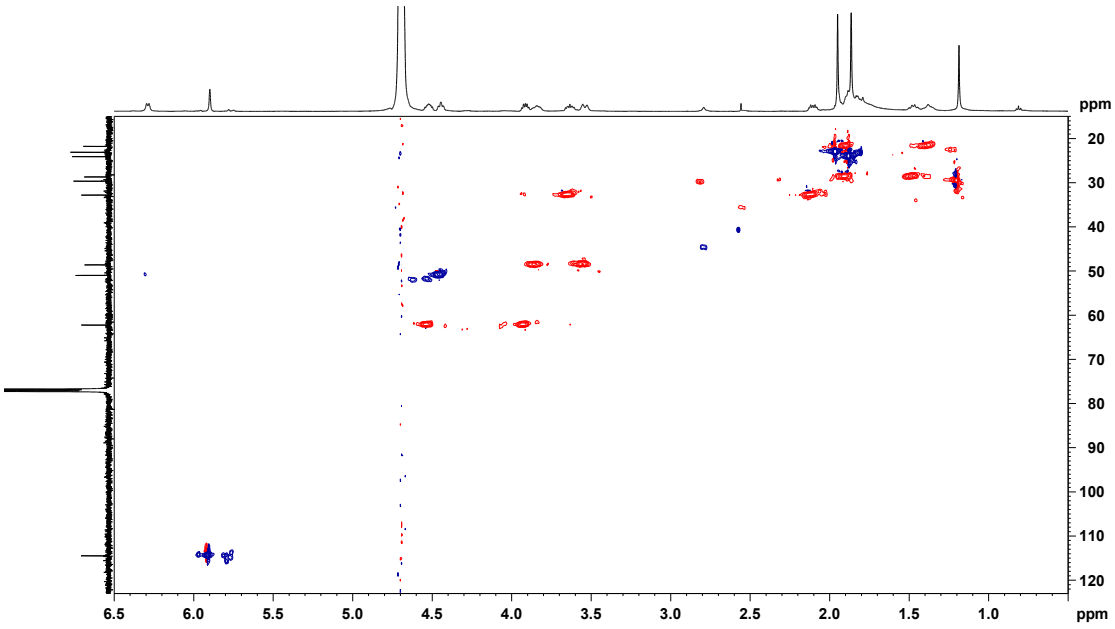

Fig. S11 HSQC spectrum of **1** (500 MHz, $CDCl_3$).

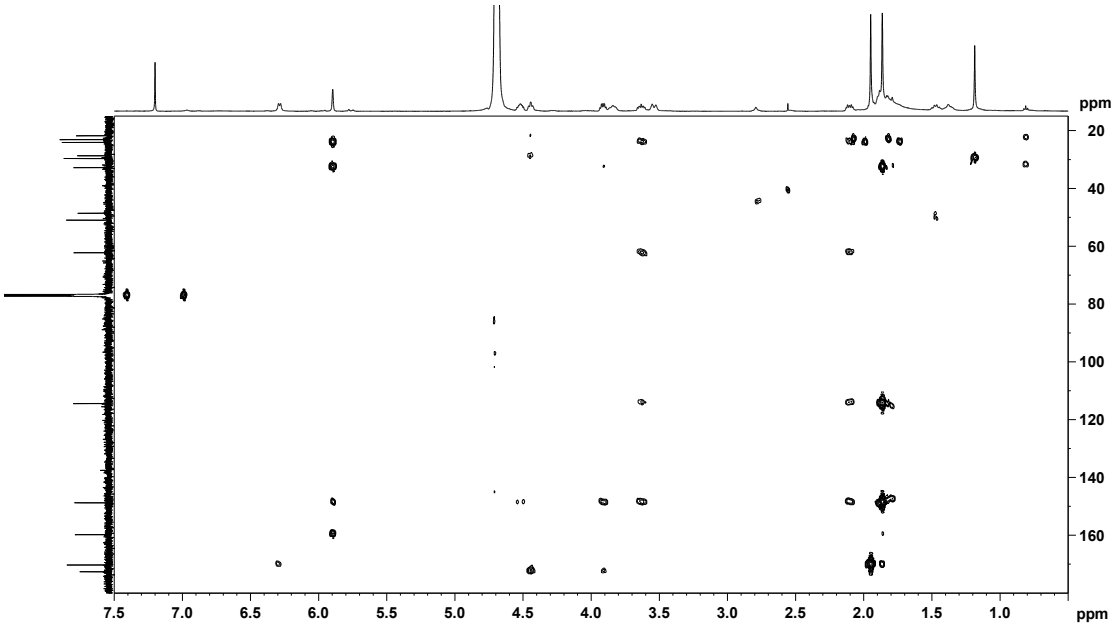

Fig. S12 HMBC spectrum of **1** (500 MHz, $CDCl_3$).

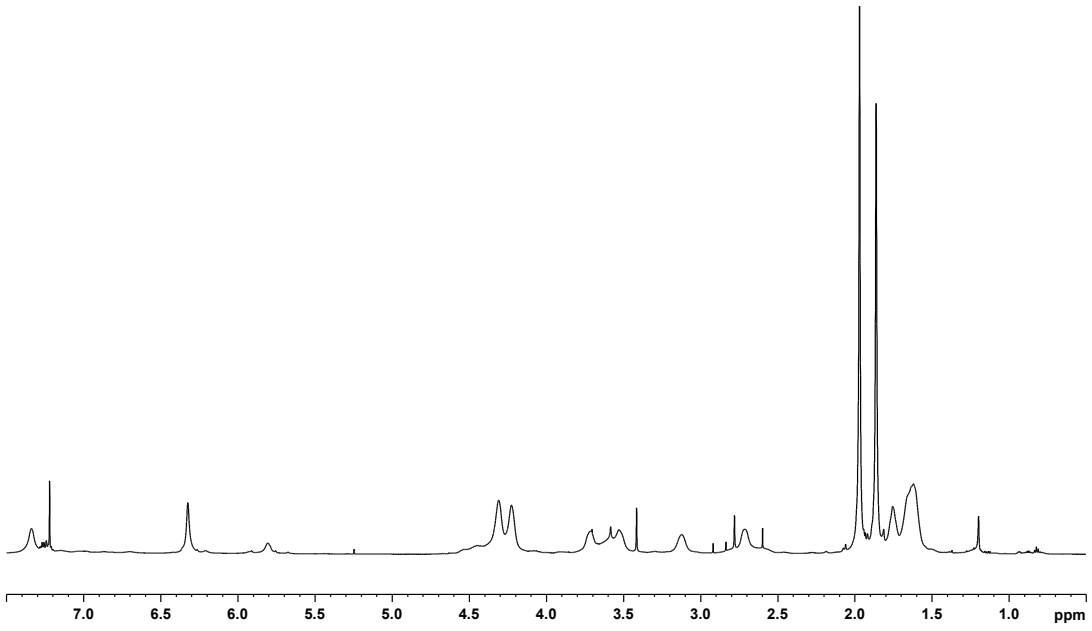

Fig. S13 ^{1}H NMR spectrum of **2** (500 MHz, $CDCl_3$).

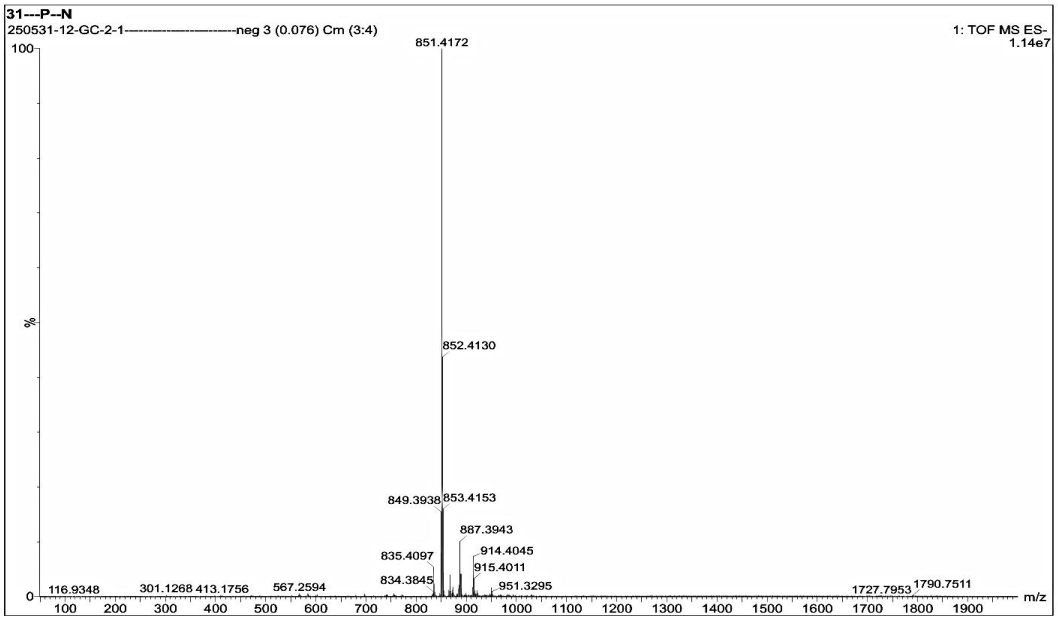

Fig. S14 TOF-MS spectrum of N,N′,N″-triacetylfusarinine C.

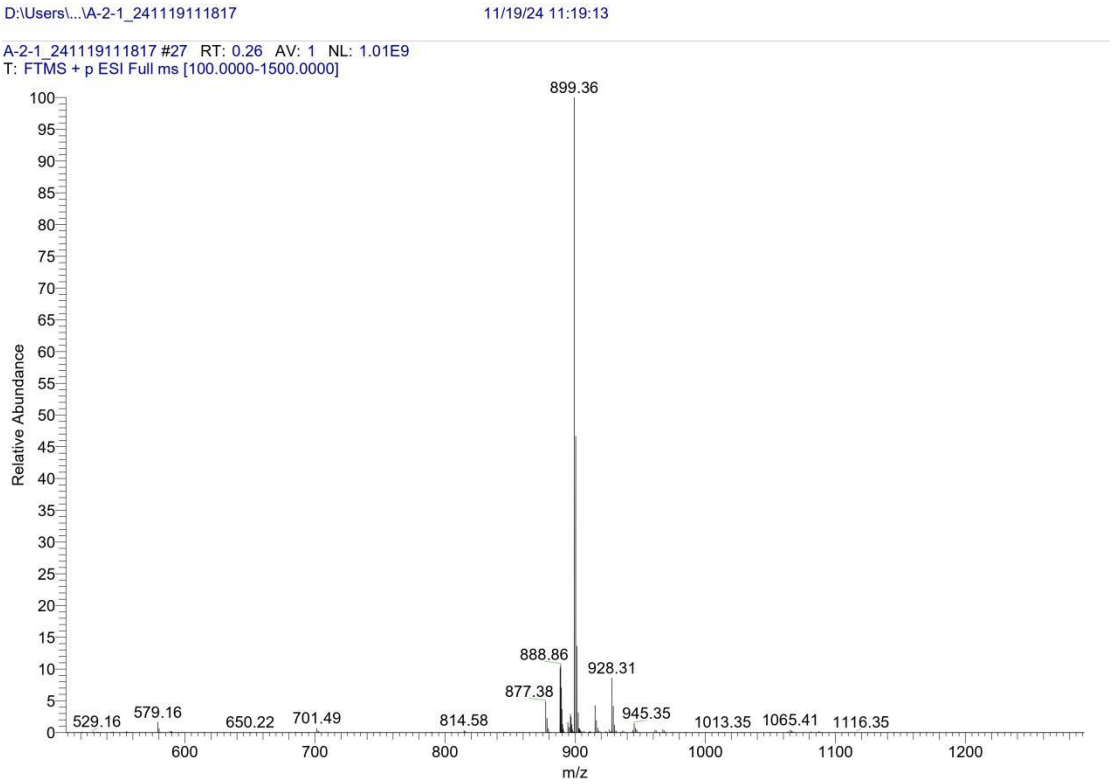

Fig. S15 TOF-MS spectrum of Al^{3+} N,N',N''-triacetylfusarinine C.

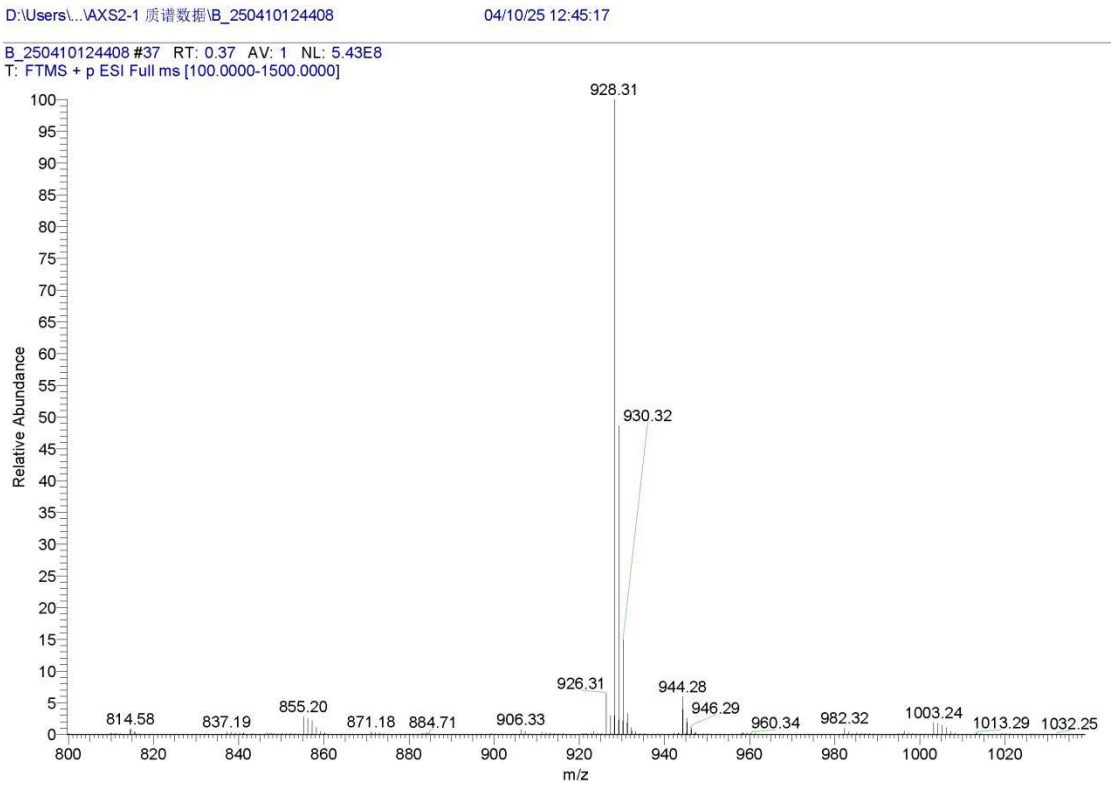

Fig. S16 TOF-MS spectrum of Fe^{3+} N,N',N''-triacetylfusarinine C.

Table S1 Physicochemical properties of copper mine wastewater.

Parameter (Unit)	Value
pH	2.85
Electrical conductivity (mS cm^{-1})	71.80
COD (mg L^{-1})	21.40
NH_4^+-N (mg L^{-1})	1.75
CO_3^{2-} (g L^{-1})	0.12
HCO_3^- (g L^{-1})	0.76
Cl^- (g L^{-1})	3.28
SO_4^{2-} (g L^{-1})	19.71
Ca^{2+} (g L^{-1})	1.67
Mg^{2+} (g L^{-1})	1.60
Na^+ (g L^{-1})	14.32
K^+ (g L^{-1})	0.19

Table S2 Metal concentrations in copper mine wastewater.

Element	Concentration (mM)	Concentration (mg L^{-1})
Cu	5.397	342.984
Fe	19.544	1091.423
Al	4.177	112.700
Mn	0.416	22.852
Zn	0.541	35.353
Pb	8.39×10^{-4}	0.174
Cr	0.0147	0.766
As	0.00617	0.462
Ni	0.028	1.646
Cd	7.10×10^{-5}	0.008

Table S3 Cu removal efficiency of *A. foveolatus* FX after 7 d of treatment under different Cu concentrations.

Cu treatment (mM)	Replicate 1 (%)	Replicate 2 (%)	Replicate 3 (%)	Removal efficiency (%)
0.5	97.20	96.90	97.23	97.11 ± 0.18
1	95.70	95.37	95.19	95.42 ± 0.26
2	92.84	93.84	89.81	92.17 ± 2.10
3	70.88	67.57	64.81	67.75 ± 3.04

Table S4 Cu removal by *A. foveolatus* FX in diluted copper mine wastewater after 7 d.

Wastewater dilution	Replicate 1 (%)	Replicate 2 (%)	Replicate 3 (%)	Removal efficiency (%)
Undiluted	0	0	0	0
2-fold dilution	41.80	39.20	36.98	39.33 ± 2.41
3-fold dilution	62.57	60.96	66.94	63.49 ± 3.09

Note: Negative removal efficiencies were recorded as 0%, indicating no net Cu removal.

Table S5 Metal removal efficiencies from copper mine wastewater by *A. foveolatus* FX after 7 days of treatment.

Metal	Replicate 1 (%)	Replicate 2 (%)	Replicate 3 (%)	Removal efficiency (%)
Cu	60.79	65.05	63.35	63.06 ± 2.14
Zn	62.37	73.87	70.41	68.88 ± 5.90
Mn	77.69	85.91	71.77	78.46 ± 7.10
Fe	88.38	85.24	90.43	88.02 ± 2.62
Al	74.08	81.24	77.29	77.54 ± 3.58

References

Huang Z-H, Liang X, Qi S-H (2020) A new iron(III) chelator of coprogen-type siderophore from the deep-sea-derived fungus *Mycosphaerella* sp. SCSIO z059. Chin J Nat Med 18(4):243–249. https://doi.org/10.1016/s1875-5364(20)30029-7

Novák J, Sokolová L, Lemr K, Pluháček T, Palyzová A, Havlíček V (2017) Batch-processing of imaging or liquid-chromatography mass spectrometry datasets and de novo sequencing of polyketide siderophores. Biochim Biophys Acta Proteins Proteom 1865(7):768–775. https://doi.org/10.1016/j.bbapap.2016.12.003

Walsh JP, DesRochers N, Renaud JB, Seifert KA, Yeung KKC, Sumarah MW (2021) Identification of N,N′,N″-triacetylfusarinine C as a key metabolite for root rot disease virulence in American ginseng. J Ginseng Res 45(1):156–162. https://doi.org/10.1016/j.jgr.2019.08.008